

# Polymer Chemistry

Volume 16  
Number 23  
21 June 2025  
Pages 2695-2792

rsc.li/polymers



ISSN 1759-9962



## PAPER

Alaitz Ruiz de Luzuriaga *et al.*  
Dynamic by design: unlocking full relaxation in disulfide epoxy networks

**15**  
YEARS  
ANNIVERSARY

Cite this: *Polym. Chem.*, 2025, **16**,  
2701

## Dynamic by design: unlocking full relaxation in disulfide epoxy networks†

Paula Fanlo, <sup>a,b</sup> Osman Konuray, <sup>c</sup> Olaia Ochoteco,<sup>a</sup> Marta Ximenis,<sup>b</sup> Alaitz Rekondo,<sup>a</sup> Hans Jürgen Grande,<sup>a,d</sup> Xavier Fernández-Francos, <sup>c</sup> Haritz Sardon <sup>b</sup> and Alaitz Ruiz de Luzuriaga <sup>\*a</sup>

Aromatic disulfide-containing epoxy networks offer a promising approach to achieving sustainable materials due to their repairable, recyclable, and reprocessable properties. However, in all cases, an excess of hardener is required to achieve full reparability. In this study, a theoretical analysis demonstrates that when aromatic disulfide is incorporated into the amine hardener, the resulting epoxy vitrimer does not fully relax due to epoxy group homopolymerization, which leads to the formation of non-dynamic crosslinks. To overcome this limitation, an epoxy monomer containing disulfide bonds was synthesized. This monomer enables complete relaxation, as the homopolymerized epoxy system also contributes to the formation of dynamic crosslinks. Using this new monomer, epoxy vitrimers were prepared that can relax without requiring an excess of amine. However, these materials exhibit inferior properties compared to those prepared with an aromatic disulfide-based diamine. To enhance their properties, a non-dynamic epoxy was introduced into the formulation. Both experimental and computational results demonstrate that up to 32% of non-dynamic epoxy can be incorporated without compromising dynamic features such as repairability, reprocessability, and recyclability, making this system significantly more suitable for industrial implementation.

Received 7th February 2025,  
Accepted 10th April 2025DOI: 10.1039/d5py00124b  
rsc.li/polymers

### 1. Introduction

Dynamic chemistry is a rapidly advancing field focused on harnessing reversible chemical reactions to create adaptable materials.<sup>1–9</sup> This approach is based on the principle of reversibility, enabling specific chemical bonds to break and reform under controlled conditions, enabling materials to adapt, repair, or regenerate themselves as needed. Vitrimers feature dynamic covalent bonds that provide structural flexibility without compromising mechanical properties.<sup>10–19</sup> The presence of dynamic covalent bonds grants vitrimers reshaping capabilities, strength, and recyclability, making them suitable

for sustainable applications.<sup>20–24</sup> By fine-tuning molecular structures and catalysts, researchers can tailor vitrimers to meet diverse performance requirements, such as enhanced toughness and flexibility. Their reversible nature also enables efficient recycling, offering a promising solution for reducing material waste. Consequently, vitrimers represent a significant innovation in materials science, delivering durable, versatile, and circular solutions across various industries.<sup>25–27</sup>

Aromatic disulfide-containing epoxy vitrimers have attracted significant attention in materials science due to their unique properties and wide-ranging applications. These vitrimers are defined by the presence of dynamic aromatic disulfide bonds, which play a crucial role in their adaptive behaviour and functionality.<sup>28–36</sup> The incorporation of these bonds enables rapid stress relaxation and moderate-temperature malleability, providing advantages in reshaping and post-processing. Notably, aromatic disulfide bonds allow for reconfiguration, recycling, and repair, enhancing both sustainability and practicality. However, achieving full recyclability and complete stress relaxation requires an excess of amine in the formulation.<sup>19</sup> It is hypothesized that without amine excess, epoxide homopolymerization becomes more favourable, leading to the formation of non-dynamic C–O bonds in the polymer backbone. These non-dynamic crosslinks hinder full relaxation, thereby limiting the material's reprocessability. Indeed,

<sup>a</sup>CIDETEC, Basque Research and Technology Alliance (BRTA), Po. Miramón 196, 20014 Donostia-San Sebastian, Spain. E-mail: aruiz@cidetec.es, haritz.sardon@ehu.eus

<sup>b</sup>POLYMAT, Department of Polymers and Advanced Materials: Physics, Chemistry and Technology, Faculty of Chemistry University of the Basque Country UPV/EHU, Joxe Mari Korta Center, Avda. Tolosa 72, 20018 Donostia-San Sebastian, Spain

<sup>c</sup>Polytechnic University of Catalonia (UPC), Thermodynamics Laboratory ETSEIB, Av. Diagonal 647, 08028 Barcelona, Spain

<sup>d</sup>University of the Basque Country (UPV/EHU), Advanced Polymers and Materials: Physics, Chemistry and Technology Department, Avda. Tolosa 72, 20018 Donostia-San Sebastian, Spain

† Electronic supplementary information (ESI) available. See DOI: <https://doi.org/10.1039/d5py00124b>



Poutrel *et al.* studied experimentally the effect of controlled epoxy excess in epoxy-carboxylic acid vitrimers and determined that the formed polyether network prevented complete stress relaxation above a certain composition threshold.<sup>37</sup>

It is well established that both the proportion and architectural distribution of dynamic bonds in vitrimers are critical in determining their mechanical properties and overall dynamism. The density of exchangeable bonds, which directly correlates with the percentage of dynamic bonds, has a significant influence on the material's dynamic behaviour.<sup>25</sup> Given that the number of successful bond exchanges affects vitrimer performance and adaptability,<sup>38,39</sup> it is essential to precisely control the percentage of dynamic bonds and their exchange rate to tailor the material's properties effectively.

The stress relaxation behaviour of a polymer network containing dynamic bonds can be analysed by drawing an analogy to a decrosslinking process, where the deactivation of network strands' elastic activity due to bond exchange is considered analogous to the reduction in crosslinking density caused by bond cleavage.<sup>40</sup> This approach has been successfully employed to determine permanent network effects and predict kinetic trends related to stress relaxation in a wide range of stepwise vitrimers.<sup>40–43</sup> To investigate how network architecture influences bond exchange dynamics and stress relaxation, it is essential to have a realistic representation of the network structure, including its repeating units, connectivity, and the distribution of dynamic and permanent bonds.<sup>40</sup> In the present system, a probable network structure can be constructed using network build-up models based on structural fragments,<sup>44</sup> combined with a kinetic model that accounts for epoxy-amine and polyetherification reactions.<sup>45–47</sup> By applying the concept of a permanent network, the effect of composition on stress relaxation and reprocessing capabilities across different polymer networks can be assessed.<sup>40</sup> The insights gained from this modelling approach can help optimize formulations by minimizing the dynamic monomer content without compromising reprocessing performance.<sup>40</sup> Other approaches are being developed from other groups like the study of the Guerre *et al.* that use different content of aromatic/aliphatic disulfides to reach the total relaxation of the network.<sup>48</sup> They achieved complete and fast relaxation by incorporating 20% mol of an aliphatic cystamine hardener beside an aromatic hardener, whereas the present study demonstrated that full relaxation can be obtained by incorporating aromatic disulfide bonds directly into the epoxy monomer. While the cited work leveraged the dynamic nature of aliphatic disulfides for rapid relaxation, the present study optimized network design to achieve relaxation without requiring amine excess, addressing the issue of non-dynamic crosslinks formed *via* epoxy homopolymerization.

In this study, we explored the dynamics of aromatic disulfide-based epoxy networks using a combined theoretical and experimental approach. To our knowledge, this is the first analysis of hybrid covalent adaptable networks (CANs) formed through the interplay of stepwise and chain-growth processes—specifically, epoxy-amine and polyetherification reactions. A

recent work by Hafner *et al.* discussed the possibility of defining disulphide-based epoxy-amine formulations with reduced dynamic monomer content,<sup>49</sup> but the percolation structural model they used was only defined for stoichiometric systems neglecting the contribution of the polyetherification. In the present work, we first examined the formation of permanent bonds due to the homopolymerization of the non-dynamic epoxy component in formulations lacking non-reacted amine. To enhance network dynamics for improved reprocessing and recycling, we synthesized a novel epoxy monomer incorporating an aromatic disulfide core. Three systems were developed, varying the location of the aromatic disulfide (in the epoxy, the amine, or both), while carefully controlling the ratio of dynamic bonds. We also investigated the role of excess amine, comparing its influence on network dynamics to that of disulfide bonds. Six formulations were analysed in terms of thermal, dynamic, and mechanical properties. Finally, we theoretically identified an optimal formulation that maximizes the incorporation of non-dynamic DGEBA to enhance mechanical properties while preserving dynamic features and validated this experimentally. This comprehensive approach offers a pathway to cost-effective and sustainable vitrimers with tailored properties.

## 2. Materials and methods

### 2.1. Material

Bis(4-hydroxyphenyl) disulfide was purchased from BLD Pharmatech GmbH (BHPDS). Epichlorohydrin (ECH), benzyl triethylammonium chloride (TEBAC), anhydrous magnesium sulfate ( $\text{MgSO}_4$ ), deuterated dimethyl sulfoxide ( $\text{DMSO-}d_6$ ), 4-amino phenyl disulfide 98% (4-AFD, DGEBA Hardener), 4,4'-methylenedianiline 97% (MDA, BGPDS hardener), dimethyl sulfoxide (DMSO) and sodium hydroxide (NaOH) were purchased from Sigma-Aldrich. Ethyl acetate (AcOEt) was purchased from Thermo Fisher Scientific. Diglycidyl ether of bisphenol A based epoxy resin (Epikote Resin EPON 828) was purchased from Westlake Epoxy. Bis(4-glycidylphenoxy) disulfide was synthesized by us. All of the products were used as received. The NMR of the both epoxies were performed to check the EEW (Fig. S3 and S4†).

### 2.2. Methods

Using  $\text{DMSO-}d_6$  as a solvent,  $^1\text{H-NMR}$  analyses were performed using an NMR spectrometer (TM 600) manufactured by Bruker Ascend, MA. 500 MHz was used to record the  $^1\text{H-NMR}$ . A differential scanning calorimeter (DSC) from TA Instruments (Discovery DSC25 Auto) was used to perform DSC measurements under nitrogen, covering a temperature range of 25 °C to 220 °C. At a scan rate of 10 and 20 °C  $\text{min}^{-1}$ , the inflection point of the heat flow step was recorded to determine the glass transition temperature ( $T_g$ ). Using TA Instruments Q500 equipment in a nitrogen environment, the thermogravimetric analysis (TGA) was carried out at a heating rate of 10 °C  $\text{min}^{-1}$  from 25 °C to 600 °C. The equipment used for the thermo-



mechanical investigations was a TA Instruments DMA Q800. The film cantilever beam was used in tension mode, and the sample films' average dimensions were  $35 \times 6 \times 1$  mm. The range of temperatures was 25 to 250 °C. The study of temperature-dependent behaviour involved tracking variations in force and phase angle while maintaining a constant oscillation frequency (1 Hz) and amplitude (15  $\mu$ m) inside a linear viscoelastic area at a heating rate of 3 °C min<sup>-1</sup>. Additionally, tensile stress-relaxation tests were conducted using a DMA Q800 device in tensile mode. To keep the samples straight, they were first preloaded with a force of  $1 \times 10^{-3}$  N. 1% of the specimens' length was stretched, and the deformation persisted throughout the test. The stress relaxation modulus was monitored and the reduction in stress was noted. Relaxation periods were calculated as the amount of time needed to relax 63% of the original stress, based on Maxwell's model for viscoelastic fluids. Using the Arrhenius eqn (1), the activation energy values  $E_a$  for each vitrimer were determined after the relaxation durations at each temperature were determined. The Arrhenius relation indicates that the topological freezing temperature ( $T_v$ ) is defined as the temperature at which the material attains a viscosity of  $10^{12}$  Pa s.

$$\tau(T) = \tau_0 e^{\frac{E_a}{RT}} \quad (1)$$

Creep tests were carried out using a DMA Q800 device in tensile mode at different temperatures (200 and  $T_g - 50$  °C) and two different stresses (0.5 MPa and 5 MPa). The samples were equilibrated for 5 minutes at corresponding temperature and then stressed for 60 minutes and recovered for another 30 minutes. An INSTRON 3365 equipped with Static Axial Clip-On Extensometer and operated with Bluehill Lite software was used to perform mechanical tests. Dumbbell type test specimens were used, and tensile strength measurements were performed in accordance with UNE-EN-ISO 527 standard, at an elongation rate of 1 mm min<sup>-1</sup>. Using different pieces of the specimens, the reprocessability of manufactured vitrimers was investigated. The specimens were warmed for five minutes at 200 °C before being hot-pressed. Following that, the heated specimens were sandwiched between two Teflon-coated metal plates and hot pressed for five minutes at 200 °C and 40 bar. Samples were demoulded once they cooled below  $T_g$ .

### 2.3. Synthesis and characterization of the formulations

#### 2.3.1. Synthesis of the bis(4-glycidyloxyphenyl) disulfide.

The synthesis of the bis(4-glycidyloxyphenyl) disulfide used in the present study was performed following a previously reported method by our group (Scheme 1).<sup>50</sup> 1 eq. of BHPDS

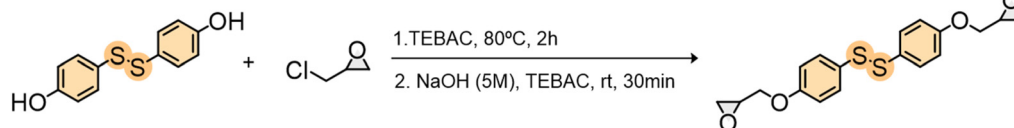
was dissolved in 10 eq. of ECH, then, 0.1 eq. of TEBAC was added, and the mixture was allowed to react under stirring for 2 h at 80 °C in air atmosphere. Subsequently, the mixture was cooled down to room temperature. 2.7 eq. of NaOH dissolved in deionized distilled water (5 M) and 0.1 eq. of TEBAC were added, and the mixture was allowed to continue reacting under stirring for 30 min at room temperature. Finally, the product was extracted with ethyl acetate and dried with MgSO<sub>4</sub> and the ECH was removed under reduced pressure using a condenser connected to a vacuum pump, obtaining the bis(4-glycidyloxyphenyl) disulfide with a 92% yield. <sup>1</sup>H-NMR (500 MHz, DMSO-*d*<sub>6</sub>,  $\delta$ ): 7.41 (m, 4H, Ar-H), 6.99 (m, 4H, Ar-H), 4.33 (dd, 2H, OCH<sub>2</sub>), 3.84 (dd, 2H, OCH<sub>2</sub>), 3.33 (m, 2H, CH in oxirane), 2.84 (dd, 2H, OCH<sub>2</sub> in oxirane), 2.7 (dd, 2H, OCH<sub>2</sub> in oxirane). <sup>13</sup>C-NMR (100 MHz, DMSO-*d*<sub>6</sub>,  $\delta$ ): 158.62 (Ar CO), 131.87 (Ar C), 127.35 (Ar CS), 115.57 (Ar C), 69.13 (OCH<sub>2</sub>), 49.57 (s, 2C, CHO in oxirane), 43.74 (s, 2C, CH<sub>2</sub>O in oxirane).

**2.3.2. Synthesis and curing process of epoxy resin with different dynamic proportion.** We studied three different epoxy vitrimer systems namely EVS1, EVS2 and EVS3 (Fig. 1). Where the dynamic disulfide is located in the different formulation components: amine, epoxy or both, respectively. Furthermore, to assess the effect of the amine excess, two different formulations were prepared for each system (1.0 eq. of amine/epoxy and 1.2 eq. of amine/epoxy) obtaining a total of 6 different formulations.

The synthesis of the epoxy networks used in the present study was performed following previously reported method by our group.<sup>51,52</sup> Briefly, the corresponding amount of the epoxy vitrimers were mixed by heating at 80 °C and degassed under vacuum (Table 1). The resultant viscous liquid was then poured between two glass plates separated by a 3 mm silicon joint and cured at 120 °C for 2.5 hours, and then post-cured at 150 °C for 2 hours. The complete curing of the epoxy vitrimers was confirmed by differential scanning calorimetry (DSC), where no residual exothermic cure peak was observed (Fig. S1†).

#### 2.3.3. Effect of non-dynamic part present in the network.

To experimentally assess the effect of the non-dynamic part on the network, we prepared 5 formulations, namely verification epoxy systems (VES\_X%), containing variable amounts of non-dynamic part (with X mol% of DGEBA) (Table 2). Following the same synthetic procedure, the corresponding amount of the epoxy mixture and amine were mixed by heating at 80 °C and degassed under vacuum. The resultant viscous liquid was then poured between two glass plates separated by a 3 mm silicon joint and cured at 120 °C for 2.5 hours, and then post-cured at 150 °C for 2 hours. The complete cure of the epoxy vitrimers was confirmed by differential scanning calorimetry



Scheme 1 Synthesis of the BGPDS.





**Fig. 1** Synthetic schemes of (a) epoxy and amine reaction and (b) polyetherification reaction. (c) Network build-up and connectivity as a function of epoxy conversion for stoichiometric EVS1 (left), and (d) relevant network parameters as a function of  $r_{\text{epoxy}}$ , the epoxy : amine ratio (bottom). When  $r_{\text{epoxy}} > 0.847$ , a non-zero residual XLD is obtained (inset). The gel point (0.57) is marked with a dashed red line.

**Table 1** Proportions for the synthesis of the 6 different formulations

| Sample | Stoichiometry (NH <sub>2</sub> /epoxy) | Part A (mol) | Part B (mol) |
|--------|--|--------------|--------------|
| ESV1   | 1.0                                    | DGEBA 0.3    | 4-AFD 0.15   |
|        | 1.2                                    | DGEBA 0.3    | 4-AFD 0.19   |
| ESV2   | 1.0                                    | BGPDS 0.28   | MDA 0.14     |
|        | 1.2                                    | BGPDS 0.28   | MDA 0.16     |
| ESV3   | 1.0                                    | BGPDS 0.28   | 4-AFD 0.14   |
|        | 1.2                                    | BGPDS 0.28   | 4-AFD 0.16   |

**Table 2** Proportions of the materials for the verification of the theoretical prediction

| Sample  | Part A (mol) |       | Part B (mol)<br>MDA |
|---------|--------------|-------|---------------------|
|         | DGEBA        | BGPDS |                     |
| VES_60% | 0.078        | 0.052 | 0.065               |
| VES_40% | 0.052        | 0.078 | 0.065               |
| VES_32% | 0.040        | 0.090 | 0.065               |
| VES_30% | 0.039        | 0.091 | 0.065               |
| VES_20% | 0.026        | 0.104 | 0.065               |

(DSC), where no residual exothermic cure peak was observed (Fig. S2†).

#### 2.4. Network build-up and stress relaxation model

Two types of polymer networks, EVS1 and EVS2, are analysed using a network build-up and stress relaxation model. In EVS1 system, dynamic bonds are incorporated in the diamine com-

ponent, while in EVS2 system, they are present in the epoxy component.

The network build-up process is modelled by defining a set of structural fragments that combine according to specific rules.<sup>44</sup> This structural model accounts for both the epoxy-amine reaction (Scheme 2a) and polyetherification (Scheme 2b).<sup>45–47,53</sup> As shown, the epoxy-amine reaction forms structures in which amine species with A<sup>+</sup> bonds are linked to epoxy species with A<sup>−</sup> bonds. Similarly, the polyetherification reaction can be represented by species with E<sup>−</sup> bonds connecting to other species with E<sup>+</sup> bonds.

The definition of structural fragments can also take into consideration the symmetry of epoxy and diamine components. Taking EVS1 as an example, by defining the internal bonds DG and S as shown in Scheme 3, the dimers can be split, providing computational facility.<sup>44</sup>

A distribution of structural fragments with varying connectivity is generated using a kinetic model, and the resulting probable network structure is analysed through well-established recursive methods.<sup>44,54</sup> Fragments with A<sup>+</sup> bonds can only combine with those containing A<sup>−</sup> bonds, and similarly, fragments with E<sup>+</sup> bonds can only pair with E<sup>−</sup> bonds. In contrast, fragments with DG bonds can randomly recombine with each other, as can fragments with S bonds. The likelihood of different combinations depends on the concentration (or number) of these bonds at a given time.

The pre-gel network formation process is simulated by calculating the expected weights associated with each bond type at a



## a) Epoxy-amine reaction



## b) Polyetherification

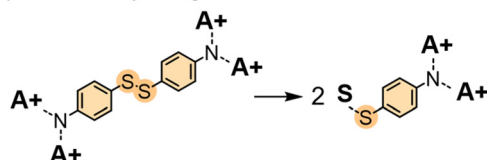


**Scheme 2** Epoxy-amine addition (a) and polyetherification (b) and the resulting structural fragments (right).

## a) Diepoxy splitting



## b) Diamine splitting



**Scheme 3** Symmetrical dimers can be split into monomeric structural fragments for ease of computation of the evolution of the structural fragments. It is modeled using a set of differential equations representing the curing kinetics which is assumed to be the same for both systems as the amine and epoxide compounds in the two systems are structurally analogous.

given curing extent (which is not considered in this analysis), while the post-gel network is examined by determining the extinction probabilities of each bond type.<sup>44</sup> The extinction probability of a given bond type,  $Z_i$ , is the likelihood that a finite branch originates from this bond outward. The crosslinking density (XLD) is then determined based on the probability that the different bonds have infinite continuation,  $1 - Z_i$ .

To evaluate the reprocessing capabilities of the different networks, we apply the permanent network concept.<sup>40,55</sup> Dynamic bonds are entirely removed from the system, and the recursive method is employed to assess the presence of residual XLD. This residual XLD is used to estimate the fraction of residual stress during a stress relaxation process and to determine the threshold composition required for full stress relaxation and complete reprocessing capabilities. For the EVS1 system, the influence of the epoxy-amine ratio is analysed, while for the EVS2 system, we investigate the feasibility

of replacing a fraction of the dynamic epoxy monomer with a conventional, non-dynamic epoxy monomer.

A comprehensive definition of structural fragments, along with a detailed description of the model mechanics and recursive computation procedures, can be found in the ESI,<sup>†</sup> which also includes the full definition of the structural fragments for both systems.

## 3. Results

### 3.1. Network build-up and stress relaxation model outputs using aromatic amine disulfide

As previously reported, conventional aromatic disulfide epoxy vitrimers with dynamic bonding provided by the amine part (EVS1), which do not contain excess amine in their formulation, are unable to fully relax due to the small amount of permanent bonds present in the network (Fig. 1).<sup>19,35,52,56</sup> This limitation poses challenges for reprocessing, repairing, and recycling these materials. To confirm that these non-permanent bonds are attributed to the homopolymerization of the DGEBA (non-dynamic) part, the following theoretical model was designed. The network build-up process is modelled by defining a set of structural fragments that combine according to certain rules.<sup>44</sup> This structural model takes into consideration the epoxy-amine reaction (Scheme 2a) and polyetherification (Scheme 2b).<sup>45–47,53</sup> As shown, the epoxy-amine reaction leads to the formation of structures where amine species with  $A^+$  bonds are connected to epoxy species with  $A^-$  bonds. It can also be seen that the polyetherification reaction is represented by species with  $E^-$  bonds that are connected to other species with  $E^+$  bonds.

The model outputs for the EVS1\_1.0 system are summarized in Fig. 2. The network build-up process of a stoichiometric epoxy-amine system is represented in Fig. 2a. As observed, the simultaneous occurrence of epoxy-amine and



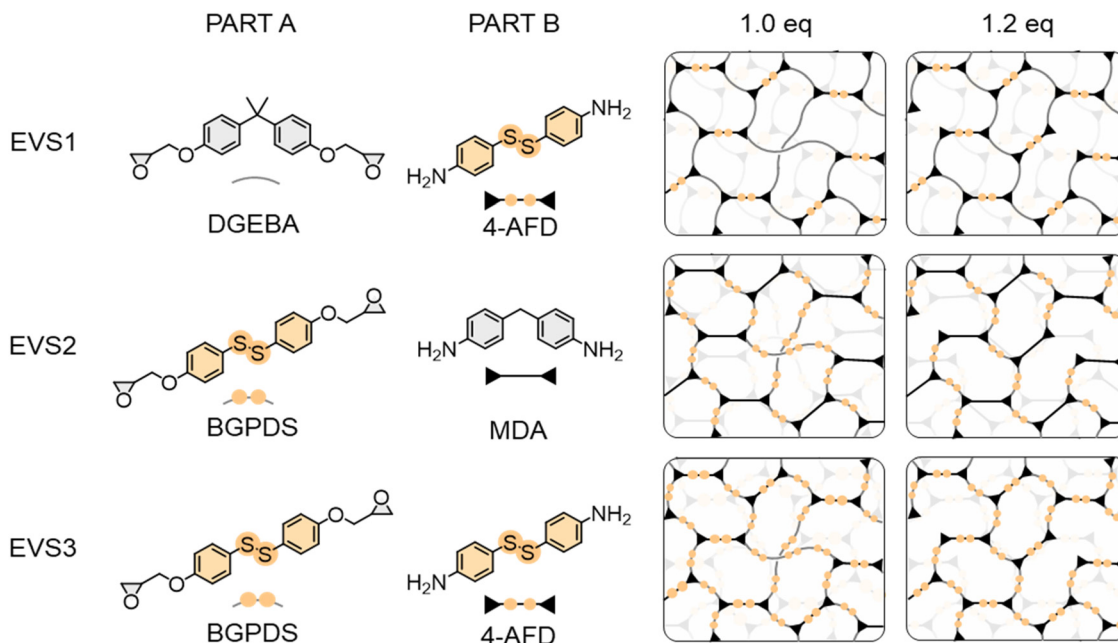


**Fig. 2** Studied three epoxy vitrimer systems (EVS). Formulations (left) and schematic representations of the corresponding stoichiometric and non-stoichiometric networks.

etherification reactions is correctly captured. Polyetherification becomes relevant once the epoxy-amine reaction has formed a significant number of hydroxyl groups, eventually leading to 15% etherified epoxy groups and, therefore, a fraction of unreacted amines. The crosslinking density (XLD) begins to increase once the gel point is reached at an epoxy conversion of 0.57 (Fig. 1, left) which is slightly lower than the predicted value of 0.58 based on the Flory–Stockmayer relation for an ideal A4–B2 system where polyetherification is not considered.

For the cured network to fully relax, no permanent network structure should remain after all the dynamic bonds have been cleaved. This is simulated by removing all disulfide bonds and calculating the residual XLD by dividing the XLD of the cleaved network by that of the original network. As seen in Fig. 1a, a residual XLD becomes apparent once etherification has occurred to a certain extent (above an epoxy conversion of 0.9). The final residual XLD is 0.16, suggesting that a significant permanent network remains after curing, which would limit the reprocessability of the stoichiometric material.

To analyse the effect of composition, the residual XLD for a wide range of epoxy:amine ratios has been calculated, along with the fraction of etherified epoxy and the fraction of reacted amines (Fig. 1b, bottom). It can be observed that there is a threshold epoxy:amine ratio ( $r_{\text{epoxy}} = 0.847$ ) below which no residual XLD is present in the cured material. Additionally, polyetherification occurs even at epoxy:amine ratios as low as 0.5, albeit at a limited rate. As expected, as  $r_{\text{epoxy}}$  increases, the fraction of polyethers in the cured network also increases, leading to increasing residual XLD at ratios higher than the reference value.

These results identify the polyether network as the main factor inhibiting the network's dynamicity in EVS1, necessitat-

ing the use of an excess of the dynamic amine component to achieve a material with full dynamic capabilities.

### 3.2. Redesigning aromatic disulfide epoxy vitrimers: importance of placing the aromatic disulfide in the correct place

It is clear that aromatic disulfides are ideal synthetic targets for obtaining high- $T_g$  epoxy vitrimers with fast reprocessability. However, incorporating the aromatic disulfide into the hardener may not be the best choice due to the significant presence of homopolymerization in the absence of excess amine. We hypothesize that incorporating the aromatic disulfide into the epoxide could potentially avoid issues related to homopolymerization. Therefore, we propose a novel system, EVS2, which incorporates BGPDS, introducing dynamic disulfide bonds within the epoxy component (Fig. 2). This design increases the density of dynamic bonds, enhancing the versatility to pair with various hardeners. To validate this hypothesis, we performed the curing process and the synthesis as in EVS1 system. Briefly, the corresponding amount of the epoxy mixture and amine were mixed by heating at 80 °C and degassed under vacuum and then cured at 120 °C for 2.5 hours, and then post-cured at 150 °C for 2 hours. In this study, we used MDA, a structural analogue of 4-AFD, as the curing agent. The curing process was confirmed by DSC (Fig. S1†). Additionally, we compared these two systems with EVS3, which integrates disulfide-containing monomers in both parts A and B: the epoxy (BGPDS) and the hardener (4-AFD) to investigate the combined contributions of these dynamic components. The properties of EVS1, EVS2, and EVS3 were analysed under two different conditions with and without an excess of amine, evaluating their thermal, dynamic, and



mechanical characteristics to understand the effects of the formulations comprehensively.

### 3.3. Thermal properties

The thermal characteristics of epoxy networks are influenced by structural and compositional elements such as cross-linking, interchain cohesive forces, and the stiffness of polymer segments.<sup>57</sup> Thus, by altering the polymer formulation, and consequently their structure, different glass transition temperature and thermal stability are expected. Hence, thermal analysis in this study includes  $T_g$  from differential scanning calorimetry and dynamic mechanical analysis, and degradation temperature obtained by thermogravimetric analysis. A close analysis on the  $T_g$  values obtained, reveals a decreasing trend from ESV1 (166 °C) to ESV2 (149 °C) and ESV3 (136 °C), respectively. We surmise that there is monomer effect caused by the flexibility presented in the phenyl S-S bonds, so, when compared to CC bonds, the dynamic phenyl S-S bond shows greater flexibility, resulting in increased mobility and a lower  $T_g$ .<sup>58,59</sup> Such trend repeats for the formulations containing an amine excess ESV1\_1.2 (152 °C) to ESV2\_1.2 (131 °C) and ESV3\_1.2 (115 °C) which is consistent with the increase of the chain mobility as a higher proportion of flexible groups is introduced in the formulations due to the decrease in the crosslinking density.

As shown below (Fig. 3 and Table S1†) the  $T_g$  values decrease when the amount of disulfide bond increases, obtaining higher  $T_g$  in EVS1 (166 and 152 °C) than EVS2 (149 and 131 °C) and EVS3 (136 and 115 °C). The ratio of epoxy monomer to diamine hardener was changed in all systems from 1.0 to 1.2, resulting in a decrease of approximately 20 °C in the  $T_g$  value in all cases.

To determine the thermal stability of epoxy vitrimers that were synthesized, thermogravimetric tests were performed. According to the TGA results (Fig. 3) the temperature ranges, when the weight loss was 5%, were 290 °C, 280 °C, 268 °C, 255 °C, and 253 °C. The TGA profiles showed that lower degradation temperatures were associated with higher contents of aromatic disulfide bonding, which was explained by lower energetic stability of disulfide bonding (Table S1 and Fig. S6†).<sup>60–64</sup> Thus, the increase on disulfide content seems to lead to a reduction in thermal stability.

It is acknowledged that disulfide bonds have a lower energetic stability,<sup>60–64</sup> the results from the TGA analyses in Fig. 3 (see also Table S1 and Fig. S7†) showed that higher the disulfide content lower is the thermal stability of the networks. In the 3 systems, decrease in the crosslinking density, produced by the use of a controlled excess of the amine, reduces the thermal stability in all cases, regardless of whether concentration of disulfide bonds in the material increases or decreases.



**Fig. 3** Schematic representation of the 1.0 and 1.2 formulated networks and the corresponding DSC (with  $T_g$  insets) and TGA (with  $T_{d5\%}$  insets) traces. (a) EVS1, (b) EVS2 and (c) EVS3.



### 3.4. Thermodynamic and dynamic properties

From the temperature ramp and stress relaxation at different temperatures tests of the materials various concepts were calculated, such as, the crosslink density ( $\nu_C$ ), the average molecular weight between crosslinks ( $M_{WC}$ ), activation energy ( $E_a$ ) and the topology freezing temperature ( $T_v$ ).

The rubbery modulus of vitrimers is a critical parameter that reflects their unique viscoelastic behaviour, influenced by dynamic covalent crosslinks.<sup>65</sup> At low temperatures, vitrimers exhibit a high elastic modulus, but as the temperature increases, similar to conventional thermoset materials, vitrimers undergo a gradual transition from a glassy, rigid state to a rubbery elastomeric phase. This transformation occurs over a specific temperature range, known as the glass transition temperature ( $T_g$ ).<sup>64</sup> In the rubbery state, vitrimers gradually dissipate stress through bond exchange reactions, allowing the system to achieve its lowest energy configuration and thus allowing the reshaping of the materials. A lower rubbery modulus indicates that a material is softer and more flexible in its rubbery state, requiring less force to deform and exhibiting greater chain mobility compared to materials with a higher modulus.<sup>66</sup> In vitrimer materials, especially in the ones with fast exchange kinetics a lower rubbery modulus does not always indicate a lower crosslinking density. When the exchange rate is comparable to or faster than the test frequency, the vitrimer material could behave like a viscoelastic material and the apparent rubbery modulus could decrease in spite of having high crosslinking density which is the case in aromatic disulfides. Indeed, the rubbery plateau modulus can decrease without a reduction in crosslink density. This occurs because bond exchange enables stress relaxation at timescales relevant to the measurement, leading to a reduced measured modulus. Therefore, in those cases the rubbery plateau is highly affected by both the crosslinking density and the number of dynamic bonds which does not happen in traditional thermosets where only crosslinking density impacts into the rubbery plateau. Table 3 shows that systems with an excess of amine have a lower rubbery modulus, which makes the materials more flexible than those with the corresponding 1.0 eq. formulation. We surmise that this stoichiometric imbalance results in a less crosslinked network and therefore greater flexibility and chain mobility. EVS2 exhibits the highest rubbery modulus among the three materials, followed by EVS1, with EVS3 showing the lowest value. The fact that the

vitrimer with higher dynamic bond content in Part A (EVS2) presents higher rubbery modulus than the one where dynamic bonds are in the hardener (EVS1) suggests that also the network structure and dynamic bond distribution significantly affect mechanical behaviour. The low value observed in EVS3 system can be attributed to the high concentration of dynamics bonds in the system. The swelling tests and gel content be performed on each sample to see the effect of soluble fraction. These experiments (Table S4†) shows that samples with amine excess generally exhibit lower gel content, higher swelling degrees, in accordance with the reduced rubbery plateau modulus compared to their 1.0 counterparts. This suggests that the presence of excess amine in the formulation leads to a less tightly crosslinked network, resulting in decreased mechanical strength and increased solvent uptake. Despite its low gel content, EVS3\_1.2 shows a relatively low swelling degree compared to other samples, suggesting that factors beyond crosslink density—such as heterogeneity—may be limiting its ability to absorb solvent, or due to the high gel content and low modulus could part of the sample be dissolved in the solvent.

As stated above, due to the high density of dynamic bonds, the observed rubbery modulus can be lower than expected despite having high crosslinking density. This hierarchy in rubbery modulus suggests that EVS2 possesses the greatest stiffness and resistance to deformation in its rubbery state, likely due to a higher crosslink density or more restricted chain mobility of the components in the stiffer components in the formulation. EVS1, with its intermediate rubbery modulus, strikes a balance between rigidity and flexibility. In contrast, EVS3, having the lowest rubbery modulus, is expected to be the most compliant and easiest to deform of the three materials. These differences in rubbery moduli can significantly influence the materials' mechanical properties, processability, and potential applications, with EVS2 potentially offering superior dimensional stability at elevated temperatures, while EVS3 might provide enhanced flexibility and ease of processing.

A second parameter that has been determined is the crosslinking density. It is a critical parameter as it influences the mechanical properties, thermal stability, and swelling behaviour of the polymer.<sup>67,68</sup> According to the rubbery modulus and rubber elasticity theory, (Table 3) we observed that the systems with amine excess exhibit lower  $\nu_C$  resulting in more flexible materials than the corresponding 1.0 eq. formu-

**Table 3** Calculated different parameters of the six epoxy vitrimeric systems

| Sample | Stoichiometry (NH <sub>2</sub> /epoxy) | $T_{g, DMA}$ (°C) | Rubbery modulus (MPa) | Degree of crosslinking (mol m <sup>-3</sup> ) | Molecular weight between crosslinks (g mol <sup>-1</sup> ) | Activation energy (kJ mol <sup>-1</sup> ) | $T_v$ (°C) |
|--------|--|-------------------|-----------------------|---|--|---|------------|
| EVS1   | 1.0                                    | 170               | 28                    | 2660  | 457  | 233                                       | 169        |
|        | 1.2                                    | 149               | 22                    | 1920  | 587  | 156                                       | 112        |
| EVS2   | 1.0                                    | 150               | 36                    | 3203  | 376  | 211                                       | 137        |
|        | 1.2                                    | 132               | 25                    | 2473  | 549  | 201                                       | 134        |
| EVS3   | 1.0                                    | 137               | 26                    | 2378  | 561  | 180                                       | 116        |
|        | 1.2                                    | 123               | 13                    | 1512  | 876  | 166                                       | 99         |



lation.<sup>69</sup> This is due to the non-reacted amine present in the 1.2 eq. networks that decrease the crosslink density of the samples and suggests notable differences in their network structures. According to the rubber elasticity theory, EVS2 exhibits the highest crosslink density, followed by EVS1, while EVS3 has the lowest.<sup>70</sup> This hierarchy suggests that EVS2 is the most rigid and mechanically robust, likely displaying higher stiffness and thermal stability. In contrast, EVS3, with its lower crosslink density, is expected to be more flexible and easier to process but may exhibit reduced mechanical strength and chemical resistance.<sup>67,71</sup> EVS1, sitting in between, balances rigidity and flexibility, offering intermediate properties. These variations highlight the impact of crosslink density on the physical and functional behavior of the materials.<sup>68,69</sup> As it has been discussed above the calculation of crosslink density in vitrimers using rubber elasticity theory is less accurate than in classical thermosets due to the presence of dynamic bonds, which can lead to a decrease in the rubbery plateau.

To assess the dynamicity of the EVS, stress-relaxation experiments at different temperatures were performed, finding that all systems exhibited linearity and followed Arrhenius

equation within the temperature range studied. As expected, the activation energy for the non-stoichiometric networks was lower than the corresponding stoichiometric counterparts. This is in agreement with the base-catalyzed promotion of the disulfide exchange,<sup>52,72</sup> resulting in materials with lower temperature dependency.

To study the effect of the location of the dynamic moiety in the network component, we selected a representative temperature for stress relaxation experiments, 200 °C, and compared the different behaviours for each stoichiometric EVS (Fig. 4 and 5). As first hypothesized, EVS1 is not able to fully relax, as evidenced by a plateau around 0.2, which we attribute to the homopolymerization of the epoxy part. Interestingly, when incorporating the dynamic moiety into the epoxy part (EVS2), the network is able to fully relax (green). This suggests that even if homopolymerization occurs, the presence of dynamic disulfides in the epoxy component allows the dynamic exchange in the whole network. Consequently, the presence of disulfides in both parts, EVS3, leads also to full relaxation (pink).

The relaxation times are direct indicators of the dynamicity of each system. Faster times are obtained for EVS3, then EVS2 and EVS1, respectively. This is consistent with the dynamic disulfide content (100%, 66% and 33%, respectively) but is also influenced by the intrinsic network characteristics already discussed above, with key factors like chain mobility, crosslinking degree or rubbery modulus.

The non-stoichiometric systems exhibited two distinct behaviours. For both EVS1 and EVS3, the excess amine leads to faster relaxation times, from 77 s to <5 s and 6 s to <5 s, respectively. Such trait is in agreement with (i) an increase of dynamic disulfide content in the formulation (from 33% to 38% for EVS1) and (ii) the disulfide bond exchange activation by the basic amine. Interestingly, EVS2 exhibited the opposite trend: the formulation with amine excess showed similar relaxation times compared to its stoichiometric counterpart (25 and 27s, respectively). In this system, the dynamic disulfide is present in part A (the epoxy), and increasing the amine to 1.2 equivalents reduced the dynamic proportion in the formulation (from 66% to 63%), which could explain the longer relaxation times for the system containing an amine excess. Noticeably, even though the epoxy part is dynamic, it seems that the amine excess that would promote the basic-catalysed



Fig. 4 Normalized curves of stress relaxation at 200 °C of the stoichiometric systems.



Fig. 5 Normalized curves of stress relaxation at 200 °C of (a) EVS1 (b) EVS2 and (c) EVS3 for 1.0 and 1.2 stoichiometries studied.



disulfide exchange is not so noticeable as in the counterpart EVS1.

To gain a deeper understanding of the dynamic behaviour of all the systems, we conducted creep resistance tests on the materials above and below  $T_g$ . It is well known that highly dynamic materials tend to exhibit greater strain when exposed to stress, with minimal recovery at temperatures exceeding their glass transition temperature.<sup>73–77</sup> For that purpose, creep testing was carried out in two stages. In the first, the sample is subjected to a constant stress of 0.5 MPa or 5 MPa at the corresponding temperature to observe the deformation; in the second, the recovery is recorded without applying any stress. Upon deeper analysis of the test results, it becomes evident that the creep above  $T_g$  increases as the amount of disulfide bonds rises. From 11% (EVS1\_1.0) of final deformation up to around 27% (EVS3\_1.0). In other words, materials with a higher concentration of disulfide bonds exhibit greater dynamism, making them easier to deform and maintain this defor-

mation. On the other hand, at temperatures below  $T_g$ , all samples exhibit a final strain of less than 0.5%. Based on Fig. 6, it can be concluded that none of the samples show creep at lower temperatures. In summary, all formulations demonstrate excellent creep resistance, characterized by high strain above  $T_g$  and negligible creep below  $T_g$ . Additional data and details are provided in the ESI (Table S5†).

### 3.5. Reprocessability

Vitrimers are known for their ability to be reshaped and recycled while maintaining the desired chemical and mechanical properties of crosslinked polymers, making them a focus of recent research.<sup>78–80</sup> The reprocessing conditions were consistent across all systems. Each sample was broken and then subjected to heat and pressure (40 bar at 200 °C for 5 minutes). In all cases, the samples were successfully rejoined into a single piece. However, as shown in Fig. 7, significant differences between the samples were observed, attributed to the dynamic

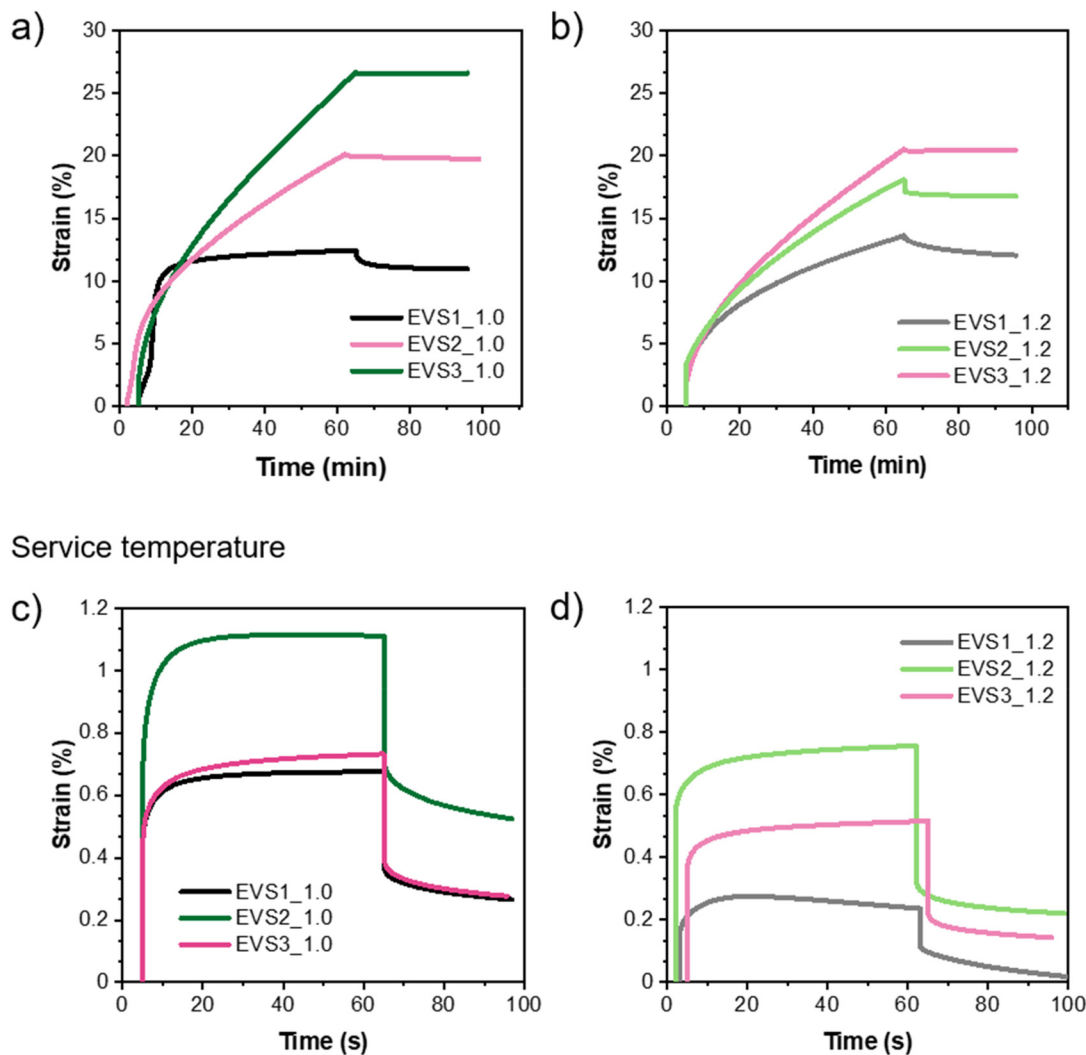


Fig. 6 Creep recovery test above  $T_g$  (200 °C and 0.5 MPa) for (a) 1.0 formulation and (b) 1.2 formulations and below  $T_g$  ( $T_g$ -50 °C and 5 MPa) for (c) 1.0 formulation and (d) 1.2 formulations.





Fig. 7 Reprocessing scheme for the different materials. Resulting films for each formulation (b) EVS1, (c) EVS2 and (d) EVS3.

nature of the systems. Generally, systems with a higher content of dynamic bonds exhibited better reprocessability, resulting in more cohesive and unified films, consistent with the DMA and stress-relaxation data. The degradation of the samples was checked using FTIR (Fig. S15–S17†) and no-degradation in their structures was observed.

### 3.6. Mechanical properties

While disulfide bonds are known for their role in self-healing and reprocessing properties, the relationship between the amount of disulfide bonds, their location and mechanical performance is not straightforward.<sup>81,82</sup> Some studies suggest that a higher number of disulfide bonds can enhance mechanical properties in materials like polyurethane elastomers.<sup>81</sup> However, other research indicates that a trade-off may exist between self-healing capability and mechanical performance when it comes to the exchange of dynamic disulfide bonds.<sup>83</sup> Hence, tensile and flexural tests were conducted to evaluate the mechanical properties of the three epoxy systems studied herein, with the goal of determining the impact of dynamic bonds on their mechanical performance (Fig. 8). In our previous work,<sup>51</sup> we demonstrated that epoxy resin containing aromatic disulfides in the hardener, similar to EVS1 system, present similar mechanical properties to reference epoxy resins. Taking this into account, in the present study, EVS1 has been considered as the reference.

The tensile and flexural modulus in vitrimers is determined by a combination of structural and dynamic factors (Fig. S18†). By tailoring these parameters, the material's stiffness and mechanical performance can be optimized for specific applications. Not only dynamic bond content, but also crosslink density and polymer backbone structure, influence these properties. Derived from these, we also have the stress-relaxation behaviour. It is clear how the percentage of disulfide bonds significantly influences the mechanical properties, resulting in lower tensile and flexural stress as the amount of the dynamic bond increases. However, in the case of the modulus this difference is negligible, with all of the cases showing similar modulus and no significant differences. Therefore, we can conclude that materials with a higher percentage of dynamic

bonds exhibit lower tensile and flexural stress at failure. However, their tensile and flexural modulus remain unchanged, indicating that stiffness is not affected. While this suggests that dynamic bonds may influence the material's ability to deform and dissipate energy, a detailed analysis of the stress-strain curves is necessary to determine whether these materials are indeed more ductile or tough.

### 3.7. Study of the limit of BGPDS in the formulations

As previously observed, the incorporation of the aromatic disulfide into the epoxide increases the density of dynamic bonds, and in this particular case, the homopolymerization of the epoxide does not have any negative impact on the dynamic behaviour. However, the incorporation of large amounts of aromatic disulfide decreases substantially the mechanical properties and more importantly, due to the high cost of this monomer, the prepared resins are not cost-effective. We hypothesize that, as in this case, since all the crosslinking points are dynamic, maybe we could potentially reduce the amount of dynamic aromatic disulfide and still keep the full dynamism through all the networks. To do so we envision that we can replace part of the aromatic disulfide containing diepoxide, with a commercial non-dynamic epoxide such as DGEBA (Fig. 9). Before starting to test different proportions, we resorted to theoretical methods to assess the limit where the network is fully dynamic, achieving the best dynamic properties, while incorporating the highest amount of DGEBA to improve mechanical properties in a cost-effective manner.

As explained in section 3.1., to evaluate the reprocessing capacities of various networks, we utilize the permanent network concept.<sup>40,55</sup> For this particular system, when a stoichiometric formulation is considered, it is of interest to know the extent to which the dynamic BGPDS component can be replaced by its non-dynamic counterpart, DGEBA, without sacrificing reprocessability. The definition of structural fragments, and the kinetic-structural model are provided in the ESI.† In Fig. 10 the residual XLD is plotted as a function of the dynamic epoxy molar fraction, defined as  $f_d$  (see the ESI† for its use in the model). As can be seen, the model simulations reveal that the dynamic monomer fraction should be kept





Fig. 8 Comparison of the mechanical properties of the six formulations studied herein. Tensile stress for (a) 1.0 formulation and (b) 1.2 formulation. Flexural stress for (c) 1.0 formulation and (d) 1.2 formulation.



Fig. 9 Formulation of VES with varying contents of DGEBA and the schematic representation of the resulting stoichiometric network.

above 0.68 to ensure no residual XLD remains. In other words, the model predicts that the dynamic epoxy can be substituted by up to 32% (mol/mol) of its non-dynamic counterpart without sacrificing the reprocessability.

To corroborate this method and to obtain an optimal material, 5 different formulations were synthesized (VES\_60%, VES\_40%, VES\_32%, VES\_30% and VES\_20%) and analysed the dynamic properties by DMA by observing the stress relaxation at 200 °C. We envision that the materials with <32% mol of non-dynamic bonds must relax totally while the others have enough permanent bonds to have a gap between the stress relaxation curve and the 0.

Indeed, the results shown in Fig. 11 are in full agreement with the theoretical model presented. First, the curve shows a complete relaxation in the formulations with less than 32 mol% DGEBA and second, a significant amount of permanent bonds (>6%) in the formulations with more than 32 mol% DGEBA were observed. Thus, the theoretical model proposing that the optimal formulation without excess amine with the best dynamic and mechanical properties is the formulation with 32% mol DGEBA, 68% mol BGPDS and 1.0 eq. of MDA, is verified. The relaxation times were also fitted to KWW model, to observe the fitting and the relaxation times distribution (Fig. S19†) and from the model information we could





**Fig. 10** Decrease in fractional residual crosslinking density as a function of dynamic epoxy molar fraction. Theoretically, the material is fully reprocessable if no residual crosslinking remains.

extract that the VES\_60% formulation exhibits more non-dynamic crosslinks, leading to a rigid, stable structure with slower relaxation and a more uniform relaxation process (indicated by a lower stretching exponent  $\beta$ ). In contrast, the VES\_20% formulation contains more dynamic crosslinks, allowing for faster, more flexible relaxation and a broader distribution of relaxation times (indicated by a higher  $\beta$ ). This behavior is characteristic of vitrimers or dynamic polymers, where reversible crosslinking enables self-healing and better processability. Thus, VES\_60% behaves more like a thermoset, offering rigidity and slow relaxation, while VES\_20% demonstrates dynamic behavior similar to dynamic polymer networks, exhibiting faster and more complex relaxation. For the rest of the samples, the corresponding behaviour was observed, increasing the relaxation time distribution (decreas-

ing  $\beta$ ) when less content of non-dynamic epoxy was added, indicating a more dynamism.

Finally, to complete the characterization and corroborate that the thermal and mechanical properties were improved compared to EVS2\_1.0, the  $T_g$  was measure by DSC having the same value as the reference EVS2\_1.0 (150 °C) and the tensile and flexural strength of this formulation (VES\_32%) were measured (Fig. 12). The new VES\_32% formulation, as expected, exhibited improved mechanical properties compared to EVS2. The differences were significantly greater, with the tensile strength increasing from 46 MPa to 56 MPa, and the flexural strength improving even more, almost doubling, from 65 MPa to 104 MPa.



**Fig. 12** Mechanical properties of VES\_32% and comparison with EVS2\_1.0.



**Fig. 11** (a) Normalized stress relaxation curve at 200 °C of the VES formulations. (b) Comparison of structural ESV systems and VES and their dynamism correlation with DGEBA content.



## 4. Conclusions

This study demonstrated that conventional epoxy vitrimer formulations based on aromatic amine containing disulfide bonds, without amine excess, fail to achieve full relaxation due to non-dynamic crosslinks formed by homopolymerization as demonstrated by permanent network modelling. We also showed that by introducing the aromatic disulfide into the epoxy monomer, it is possible to achieve full relaxation of the network as homopolymerization does not impact in the relaxation behaviour, thus maintaining their recyclability and reprocessability. Our findings show that increasing the concentration of disulfide bonds the glass transition temperature and mechanical strength decrease, resulting in a softer and more flexible material with enhanced dynamic behaviour. This trade-off allows for fine-tuning vitrimer formulations to prioritize recyclability or mechanical performance for specific applications. Interestingly, the concentration of disulfide bonds proved to have a more critical impact on vitrimer performance than the presence of amine excess, having faster relaxations without amine excess but with a higher amount of disulfide bonds than *vice versa*, further underscoring the significance of these bonds. Finally, by using theoretical methods and experimental verifications, this study also explored the integration of up to 32% of non-dynamic epoxy into formulations, which improved mechanical properties and reduced costs while retaining key dynamic features such as repairability, reprocessability, and recyclability. These findings show that understanding the system allows us to develop a customized epoxy vitrimer formulations that balance structural integrity and environmental sustainability, making them highly adaptable to a variety of industrial applications.

## Data availability

All the data will be accessible on request from the authors.

## Conflicts of interest

There are no conflicts to declare.

## Acknowledgements

HS and MX acknowledge PID2022-138199NB-I00 funded by MCIU/AEI/10.13039/501100011033. MX acknowledges the grant from the Gipuzkoa Fellows Programme (G75067454). O. Konuray and X. Fernández-Francos acknowledge the funds provided by the Spanish Ministry of Science and Innovation (MCIN/AEI/10.13039/501100011033) through R&D projects PID2020-115102RB-C22 and PID2023-147128OB-C21, and also by Generalitat de Catalunya (2021-SGR-00154). O. Konuray and X. Fernández-Francos also acknowledge the Serra-Hünter programme (Generalitat de Catalunya).

## References

- 1 J. Han, T. Liu, C. Hao, S. Zhang, B. Guo and J. Zhang, A Catalyst-Free Epoxy Vitrimer System Based on Multifunctional Hyperbranched Polymer, *Macromolecules*, 2018, **51**(17), 6789–6799, DOI: [10.1021/acs.macromol.8b01424](https://doi.org/10.1021/acs.macromol.8b01424).
- 2 H. Zheng, S. Wang, C. Lu, Y. Ren, Z. Liu, D. Ding, Z. Wu, X. Wang, Y. Chen and Q. Zhang, Thermal, Near-Infrared Light, and, Amine Solvent Triple-Responsive Recyclable Imine-Type Vitrimer: Shape Memory, Accelerated Photohealing/Welding, and Destructing Behaviors, *Ind. Eng. Chem. Res.*, 2020, **59**(50), 21768–21778, DOI: [10.1021/acs.iecr.0c04257](https://doi.org/10.1021/acs.iecr.0c04257).
- 3 W. Denissen, J. M. Winne and F. E. Du Prez, Vitrimers, Permanent Organic Networks with Glass-like Fluidity, *Chem. Sci.*, 2016, **7**(1), 30–38, DOI: [10.1039/C5SC02223A](https://doi.org/10.1039/C5SC02223A).
- 4 C. J. Kloxin, T. F. Scott, B. J. Adzima and C. N. Bowman, Covalent Adaptable Networks (CANs): A Unique Paradigm in Cross-Linked Polymers, *Macromolecules*, 2010, **43**(6), 2643–2653, DOI: [10.1021/ma902596s](https://doi.org/10.1021/ma902596s).
- 5 N. Roy, B. Bruchmann and J.-M. Lehn, DYNAMERS: Dynamic Polymers as Self-Healing Materials, *Chem. Soc. Rev.*, 2015, **44**(11), 3786–3807, DOI: [10.1039/C5CS00194C](https://doi.org/10.1039/C5CS00194C).
- 6 G. C. Tesoro and V. Sastri, Reversible Crosslinking in Epoxy Resins. I. Feasibility Studies, *J. Appl. Polym. Sci.*, 1990, **39**(7), 1425–1437, DOI: [10.1002/app.1990.070390702](https://doi.org/10.1002/app.1990.070390702).
- 7 G. M. Scheutz, J. J. Lessard, M. B. Sims and B. S. Sumerlin, Adaptable Crosslinks in Polymeric Materials: Resolving the Intersection of Thermoplastics and Thermosets, *J. Am. Chem. Soc.*, 2019, **141**(41), 16181–16196, DOI: [10.1021/jacs.9b07922](https://doi.org/10.1021/jacs.9b07922).
- 8 P. Chakma and D. Konkolewicz, Dynamic Covalent Bonds in Polymeric Materials, *Angew. Chem., Int. Ed.*, 2019, **58**(29), 9682–9695, DOI: [10.1002/anie.201813525](https://doi.org/10.1002/anie.201813525).
- 9 J. M. Winne, L. Leibler and F. E. Du Prez, Dynamic, Covalent Chemistry in Polymer Networks: A Mechanistic Perspective, *Polym. Chem.*, 2019, **10**(45), 6091–6108, DOI: [10.1039/C9PY01260E](https://doi.org/10.1039/C9PY01260E).
- 10 H. Pandya, A. Perego and F. Khabaz, Stress-induced Dynamics of Glassy Vitrimers with Fast Bond Exchange Rate, *J. Appl. Polym. Sci.*, 2024, **141**(10), DOI: [10.1002/app.55039](https://doi.org/10.1002/app.55039).
- 11 M. Guerre, C. Taplan, J. M. Winne and F. E. Du Prez, Vitrimers, Directing Chemical Reactivity to Control Material Properties., *Chem. Sci.*, 2020, **11**(19), 4855–4870, DOI: [10.1039/D0SC01069C](https://doi.org/10.1039/D0SC01069C).
- 12 V. Schenk, K. Labastie, M. Destarac, P. Olivier and M. Guerre, Vitrimer Composites: Current Status and Future Challenges, *Mater. Adv.*, 2022, **3**(22), 8012–8029, DOI: [10.1039/D2MA00654E](https://doi.org/10.1039/D2MA00654E).
- 13 F. García and M. M. J. Smulders, Dynamic Covalent Polymers, *J. Polym. Sci., Part A: Polym. Chem.*, 2016, **54**(22), 3551–3577, DOI: [10.1002/pola.28260](https://doi.org/10.1002/pola.28260).
- 14 Y. Jin, C. Yu, R. J. Denman and W. Zhang, Recent Advances in Dynamic Covalent Chemistry, *Chem. Soc. Rev.*, 2013, **42**(16), 6634, DOI: [10.1039/c3cs60044k](https://doi.org/10.1039/c3cs60044k).



- 15 M. Guerre, C. Taplan, J. M. Winne and F. E. Du Prez, Vitrimers, Directing Chemical Reactivity to Control Material Properties., *Chem. Sci.*, 2020, **11**(19), 4855–4870, DOI: [10.1039/D0SC01069C](https://doi.org/10.1039/D0SC01069C).
- 16 L. M. C. Janssen, Vitrimers: Combining the Best of Both Polymeric Worlds, *Europhys. News*, 2020, **51**(1), 4–5.
- 17 N. Markaide, A. Luzuriaga, G. Hoyos, A. Rekondo and H. Grande, Reprocessable, Repairable and Recyclable Thermoset Composites, *Rev. Mater. Compos.*, 2022, DOI: [10.23967/r.matcomp.2018.01.003](https://doi.org/10.23967/r.matcomp.2018.01.003).
- 18 A. Ruiz de Luzuriaga, N. Markaide, A. M. Salaberria, I. Azcune, A. Rekondo and H. J. Grande, Aero Grade Epoxy Vitriimer towards Commercialization, *Polymers*, 2022, **14**(15), 3180, DOI: [10.3390/polym14153180](https://doi.org/10.3390/polym14153180).
- 19 A. Ruiz de Luzuriaga, G. Solera, I. Azcarate-Ascascua, V. Boucher, H.-J. Grande and A. Rekondo, Chemical Control of the Aromatic Disulfide Exchange Kinetics for Tailor-Made Epoxy Vitrimers, *Polymer*, 2022, **239**, 124457, DOI: [10.1016/j.polymer.2021.124457](https://doi.org/10.1016/j.polymer.2021.124457).
- 20 M. Hayashi, Implantation of Recyclability and Healability into Cross-Linked Commercial Polymers by Applying the Vitriimer Concept, *Polymers*, 2020, **12**(6), 1322, DOI: [10.3390/polym12061322](https://doi.org/10.3390/polym12061322).
- 21 A. M. Hubbard, Y. Ren, D. Konkolewicz, A. Sarvestani, C. R. Picu, G. S. Kedziora, A. Roy, V. Varshney and D. Nepal, Vitriimer Transition Temperature Identification: Coupling Various Thermomechanical Methodologies, *ACS Appl. Polym. Mater.*, 2021, **3**(4), 1756–1766, DOI: [10.1021/acscapm.0c01290](https://doi.org/10.1021/acscapm.0c01290).
- 22 L. Yue, H. Guo, A. Kennedy, A. Patel, X. Gong, T. Ju, T. Gray and I. Manas-Zloczower, Vitriimerization: Converting Thermoset Polymers into Vitrimers, *ACS Macro Lett.*, 2020, **9**(6), 836–842, DOI: [10.1021/acsmacrolett.0c00299](https://doi.org/10.1021/acsmacrolett.0c00299).
- 23 M. Capelot, M. M. Unterlass, F. Tournilhac and L. Leibler, Catalytic Control of the Vitriimer Glass Transition, *ACS Macro Lett.*, 2012, **1**(7), 789–792, DOI: [10.1021/mz300239f](https://doi.org/10.1021/mz300239f).
- 24 Z. P. Zhang, M. Z. Rong and M. Q. Zhang, Polymer Engineering Based on Reversible Covalent Chemistry: A Promising Innovative Pathway towards New Materials and New Functionalities, *Prog. Polym. Sci.*, 2018, **80**, 39–93, DOI: [10.1016/j.progpolymsci.2018.03.002](https://doi.org/10.1016/j.progpolymsci.2018.03.002).
- 25 M. Chen, H. Si, H. Zhang, L. Zhou, Y. Wu, L. Song, M. Kang and X.-L. Zhao, The Crucial Role in Controlling the Dynamic Properties of Polyester-Based Epoxy Vitrimers: The Density of Exchangeable Ester Bonds, *Macromolecules*, 2021, **54**(21), 10110–10117, DOI: [10.1021/acs.macromol.1c01289](https://doi.org/10.1021/acs.macromol.1c01289).
- 26 H. Sardon, A. Pascual, D. Mecerreyes, D. Taton, H. Cramail and J. L. Hedrick, Synthesis of Polyurethanes Using Organocatalysis: A Perspective, *Macromolecules*, 2015, **48**(10), 3153–3165, DOI: [10.1021/acs.macromol.5b00384](https://doi.org/10.1021/acs.macromol.5b00384).
- 27 F. Van Lijsebetten, J. O. Holloway, J. M. Winne and F. E. Du Prez, Internal Catalysis for Dynamic Covalent Chemistry Applications and Polymer Science, *Chem. Soc. Rev.*, 2020, **49**(23), 8425–8438, DOI: [10.1039/D0CS00452A](https://doi.org/10.1039/D0CS00452A).
- 28 L. Zhong, Y. Hao, J. Zhang, F. Wei, T. Li, M. Miao and D. Zhang, Closed-Loop Recyclable Fully Bio-Based Epoxy Vitrimers from Ferulic Acid-Derived Hyperbranched Epoxy Resin, *Macromolecules*, 2022, **55**(2), 595–607, DOI: [10.1021/acs.macromol.1c02247](https://doi.org/10.1021/acs.macromol.1c02247).
- 29 Z. Ma, Y. Wang, J. Zhu, J. Yu and Z. Hu, Bio-Based Epoxy Vitrimers: Reprocessability, Controllable Shape Memory, and Degradability, *J. Polym. Sci., Part A: Polym. Chem.*, 2017, **55**(10), 1790–1799, DOI: [10.1002/pola.28544](https://doi.org/10.1002/pola.28544).
- 30 H.-Y. Tsai, T. Fujita, S. Wang and M. Naito, Environmentally Friendly Recycling System for Epoxy Resin with Dynamic Covalent Bonding, *Sci. Technol. Adv. Mater.*, 2021, **22**(1), 532–542, DOI: [10.1080/14686996.2021.1897480](https://doi.org/10.1080/14686996.2021.1897480).
- 31 D. Hong, H. Lee, B. J. Kim, T. Park, J. Y. Choi, M. Park, J. Lee, H. Cho, S.-P. Hong, S. H. Yang, S. H. Jung, S.-B. Ko and I. S. Choi, A Degradable Polydopamine Coating Based on Disulfide-Exchange Reaction, *Nanoscale*, 2015, **7**(47), 20149–20154, DOI: [10.1039/C5NR06460K](https://doi.org/10.1039/C5NR06460K).
- 32 I. Altinbasak, M. Arslan, R. Sanyal and A. Sanyal, Pyridyl Disulfide-Based Thiol-Disulfide Exchange Reaction: Shaping the Design of Redox-Responsive Polymeric Materials, *Polym. Chem.*, 2020, **11**(48), 7603–7624, DOI: [10.1039/D0PY01215G](https://doi.org/10.1039/D0PY01215G).
- 33 R. Martin, A. Rekondo, A. R. de Luzuriaga, P. Casuso, D. Dupin, G. Cabañero, H. J. Grande and I. Odriozola, Dynamic Sulfur Chemistry as a Key Tool in the Design of Self-Healing Polymers, *Smart Mater. Struct.*, 2016, **25**(8), 084017, DOI: [10.1088/0964-1726/25/8/084017](https://doi.org/10.1088/0964-1726/25/8/084017).
- 34 A. Takahashi, T. Ohishi, R. Goseki and H. Otsuka, Degradable Epoxy Resins Prepared from Diepoxide Monomer with Dynamic Covalent Disulfide Linkage, *Polymer*, 2016, **82**, 319–326, DOI: [10.1016/j.polymer.2015.11.057](https://doi.org/10.1016/j.polymer.2015.11.057).
- 35 I. Azcune, A. Huegun, A. Ruiz de Luzuriaga, E. Saiz and A. Rekondo, The Effect of Matrix on Shape Properties of Aromatic Disulfide Based Epoxy Vitrimers, *Eur. Polym. J.*, 2021, **148**, 110362, DOI: [10.1016/j.eurpolymj.2021.110362](https://doi.org/10.1016/j.eurpolymj.2021.110362).
- 36 H. Si, L. Zhou, Y. Wu, L. Song, M. Kang, X. Zhao and M. Chen, Rapidly Reprocessable, Degradable Epoxy Vitriimer and Recyclable Carbon Fiber Reinforced Thermoset Composites Relied on High Contents of Exchangeable Aromatic Disulfide Crosslinks, *Composites, Part B*, 2020, **199**, 108278, DOI: [10.1016/j.compositesb.2020.108278](https://doi.org/10.1016/j.compositesb.2020.108278).
- 37 Q.-A. A. Poutrel, J. J. Blaker, C. Soutis, F. Tournilhac and M. Gresil, Dicarboxylic Acid-Epoxy Vitrimers: Influence of the off-Stoichiometric Acid Content on Cure Reactions and Thermo-Mechanical Properties, *Polym. Chem.*, 2020, **11**(33), 5327–5338, DOI: [10.1039/d0py00342e](https://doi.org/10.1039/d0py00342e).
- 38 A. Perego and F. Khabaz, Effect of Bond Exchange Rate on Dynamics and Mechanics of Vitrimers, *J. Polym. Sci.*, 2021, **59**(21), 2590–2602, DOI: [10.1002/pol.20210411](https://doi.org/10.1002/pol.20210411).
- 39 M. Goh, H. Shin and C. B. Kim, Manipulating Bond Exchange Rates in Vitriimer Hexagonal Boron Nitride Nanohybrids via Heat Capacity Enhancement, *J. Appl. Polym. Sci.*, 2021, **138**(12), DOI: [10.1002/app.50079](https://doi.org/10.1002/app.50079).



- 40 O. Konuray, X. Fernández-Francos and X. Ramis, Structural Design of CANs with Fine-Tunable Relaxation Properties: A Theoretical Framework Based on Network Structure and Kinetics Modeling, *Macromolecules*, 2023, **56**(13), 4855–4873, DOI: [10.1021/acs.macromol.3c00482](https://doi.org/10.1021/acs.macromol.3c00482).
- 41 S. Moradi, X. Fernández-Francos, O. Konuray and X. Ramis, Recyclable Dual-Curing Thiol-Isocyanate-Epoxy Vitrimers with Sequential Relaxation Profiles, *Eur. Polym. J.*, 2023, **196**, 112290, DOI: [10.1016/j.eurpolymj.2023.112290](https://doi.org/10.1016/j.eurpolymj.2023.112290).
- 42 H. Alzubi, O. Konuray, X. Fernández-Francos, X. Ramis and S. Moradi, Easily Recycled Thiol-Ene Elastomers with Controlled Creep, *React. Funct. Polym.*, 2024, **196**, 105835, DOI: [10.1016/j.reactfunctpolym.2024.105835](https://doi.org/10.1016/j.reactfunctpolym.2024.105835).
- 43 O. Konuray, S. Moradi, A. Roig, X. Fernández-Francos and X. Ramis, Thiol-Ene Networks with Tunable Dynamicity for Covalent Adaptation, *ACS Appl. Polym. Mater.*, 2023, **5**(3), 1651–1656, DOI: [10.1021/acsapm.2c02136](https://doi.org/10.1021/acsapm.2c02136).
- 44 J.-P. P. Pascault, H. Sautereau, J. Verdu and R. J. J. Williams, *Thermosetting Polymers*, Marcel Dekker, New York, 2002.
- 45 C. C. Riccardi and R. J. J. Williams, Statistical Structural Model for the Build-up of Epoxy-Amine Networks with Simultaneous Etherification, *Polymer*, 1986, **27**(6), 913–920, DOI: [10.1016/0032-3861\(86\)90304-6](https://doi.org/10.1016/0032-3861(86)90304-6).
- 46 R. J. J. Williams, C. C. Riccardi and K. Dušek, Build-up of Polymer Networks by Initiated Polyreactions, *Polym. Bull.*, 1991, **25**(2), 231–237.
- 47 K. C. Cole, J. J. Hechler and D. Noel, New Approach to Modeling the Cure Kinetics of Epoxy Amine Thermosetting Resins. 2. Application to a Typical System Based on Bis[4-(Diglycidylamino)Phenyl]Methane and Bis(4-Aminophenyl) Sulfone, *Macromolecules*, 1991, **24**(11), 3098–3110.
- 48 S. Guggari, F. Magliozzi, S. Malburet, A. Graillet, M. Destarac and M. Guerre, Vanillin-Based Epoxy Vitrimers: Looking at the Cystamine Hardener from a Different Perspective, *ACS Sustainable Chem. Eng.*, 2023, **11**(15), 6021–6031, DOI: [10.1021/acssuschemeng.3c00379](https://doi.org/10.1021/acssuschemeng.3c00379).
- 49 B. R. Hafner, S. Pal, B. Lewis, S. Ketten and K. R. Shull, Network Topology and Percolation in Model Covalent Adaptable Networks, *ACS Macro Lett.*, 2024, **13**(11), 1545–1550, DOI: [10.1021/acsmacrolett.4c00523](https://doi.org/10.1021/acsmacrolett.4c00523).
- 50 T. Abbasoglu, O. Skarsetz, P. Fanlo, B. Grignard, C. Detrembleur, A. Walther and H. Sardon, Spatio-Selective Reconfiguration of Mechanical Metamaterials Through the Use of Dynamic Covalent Chemistries, *Adv. Sci.*, 2024, **11**(45), DOI: [10.1002/advs.202407746](https://doi.org/10.1002/advs.202407746).
- 51 A. Ruiz de Luzuriaga, R. Martin, N. Markaide, A. Rekondo, G. Cabañero, J. Rodríguez and I. Odriozola, Epoxy Resin with Exchangeable Disulfide Crosslinks to Obtain Reprocessable, Repairable and Recyclable Fiber-Reinforced Thermoset Composites, *Mater. Horiz.*, 2016, **3**(3), 241–247, DOI: [10.1039/C6MH00029K](https://doi.org/10.1039/C6MH00029K).
- 52 A. Rekondo, R. Martin, A. Ruiz de Luzuriaga, G. Cabañero, H. J. Grande and I. Odriozola, Catalyst-Free Room-Temperature Self-Healing Elastomers Based on Aromatic Disulfide Metathesis, *Mater. Horiz.*, 2014, **1**(2), 237–240, DOI: [10.1039/C3MH00061C](https://doi.org/10.1039/C3MH00061C).
- 53 L. Matějka and L. Matejka, Amine Cured Epoxide Networks: Formation, Structure, and Properties, *Macromolecules*, 2000, **33**(10), 3611–3619, DOI: [10.1021/ma991831w](https://doi.org/10.1021/ma991831w).
- 54 D. R. Miller, E. M. Valles and C. W. Macosko, Calculation of Molecular Parameters for Stepwise Polyfunctional Polymerization, *Polym. Eng. Sci.*, 1979, **19**(4), 272–283.
- 55 L. Li, X. Chen, K. Jin and J. M. Torkelson, Vitrimers Designed Both To Strongly Suppress Creep and To Recover Original Cross-Link Density after Reprocessing: Quantitative Theory and Experiments, *Macromolecules*, 2018, **51**(15), 5537–5546, DOI: [10.1021/acs.macromol.8b00922](https://doi.org/10.1021/acs.macromol.8b00922).
- 56 I. Azcune, E. Elorza, A. Ruiz de Luzuriaga, A. Huegun, A. Rekondo and H.-J. Grande, Analysis of the Effect of Network Structure and Disulfide Concentration on Vitrimer Properties, *Polymers*, 2023, **15**(20), 4123, DOI: [10.3390/polym15204123](https://doi.org/10.3390/polym15204123).
- 57 P. Fanlo, A. Ruiz de Luzuriaga, G. Albizu, M. Ximenis, A. Rekondo, H. J. Grande and H. Sardon, Unraveling the Thermal Stability of Aromatic Disulfide Epoxy Vitrimers: A Comprehensive Study Using Principal Component Analysis (PCA), *RSC Appl. Polym.*, 2024, **2**(5), 826–837, DOI: [10.1039/D4LP00156G](https://doi.org/10.1039/D4LP00156G).
- 58 K. Peng, M. Gao, Y. Yi, J. Guo and Z. Dong, Copper/Nickel-Catalyzed Selective C–S/S–S Bond Formation Starting from O-Alkyl Phenylcarbamothioates, *Eur. J. Org. Chem.*, 2020, **2020**(11), 1665–1672, DOI: [10.1002/ejoc.201901884](https://doi.org/10.1002/ejoc.201901884).
- 59 N. Xu, B. Wang, Z. An, Y. Liu, L. Liu, Z. Hu and Y. Huang, Complete Degradation of a High-Performance Epoxy Thermoset Enabled by  $\gamma$ -Ray-Sensitive Motifs Based on the Cascaded Synergetic Strategy, *Chem. Mater.*, 2022, **34**(10), 4732–4740, DOI: [10.1021/acs.chemmater.2c00728](https://doi.org/10.1021/acs.chemmater.2c00728).
- 60 F. Ruipérez, M. Galdeano, E. Gimenez and J. M. Matxain, Sulfenamides as Building Blocks for Efficient Disulfide-Based Self-Healing Materials. A Quantum Chemical Study, *ChemistryOpen*, 2018, **7**(3), 248–255, DOI: [10.1002/open.201800003](https://doi.org/10.1002/open.201800003).
- 61 W. Pawelec, A. Holappa, T. Tirri, M. Aubert, H. Hoppe, R. Pfaendner and C.-E. Wilén, Disulfides – Effective Radical Generators for Flame Retardancy of Polypropylene, *Polym. Degrad. Stab.*, 2014, **110**, 447–456, DOI: [10.1016/j.polymdegradstab.2014.09.013](https://doi.org/10.1016/j.polymdegradstab.2014.09.013).
- 62 Z. Ma, Y. Wang, J. Zhu, J. Yu and Z. Hu, Bio-based Epoxy Vitrimers: Reprocessibility, Controllable Shape Memory, and Degradability, *J. Polym. Sci., Part A: Polym. Chem.*, 2017, **55**(10), 1790–1799, DOI: [10.1002/pola.28544](https://doi.org/10.1002/pola.28544).
- 63 T. Cheng, W. Lian, W. Zhang, J. Wang, C. Wu, B. Lu, K. Tan, B. Dong, C. Liu and C. Shen, Room-Temperature Self-Repairable Yet Mechanically Robust Elastomeric Triboelectric Nanogenerators Enabled by a Fast-Reversible Dual-Dynamic Network, *ACS Sustainable Chem. Eng.*, 2023, **11**(39), 14376–14390, DOI: [10.1021/acssuschemeng.3c02399](https://doi.org/10.1021/acssuschemeng.3c02399).
- 64 S. Kim, H. Jeon, S. Shin, S. Park, J. Jegal, S. Y. Hwang, D. X. Oh and J. Park, Superior Toughness and Fast Self-



- Healing at Room Temperature Engineered by Transparent Elastomers, *Adv. Mater.*, 2018, **30**(1), DOI: [10.1002/adma.201705145](https://doi.org/10.1002/adma.201705145).
- 65 F. Meng, M. O. Saed and E. M. Terentjev, Rheology of Vitrimers, *Nat. Commun.*, 2022, **13**(1), 5753, DOI: [10.1038/s41467-022-33321-w](https://doi.org/10.1038/s41467-022-33321-w).
- 66 D. Koblar, J. Škofic and M. Boltežar, Evaluation of the Young's Modulus of Rubber-Like Materials Bonded to Rigid Surfaces with Respect to Poisson's Ratio, *J. Mech. Eng.*, 2014, **60**(7–8), 506–511, DOI: [10.5545/sv-jme.2013.1510](https://doi.org/10.5545/sv-jme.2013.1510).
- 67 P. J. Flory, Network Structure and the Elastic Properties of Vulcanized Rubber, *Chem. Rev.*, 1944, **35**(1), 51–75, DOI: [10.1021/cr60110a002](https://doi.org/10.1021/cr60110a002).
- 68 X. Zheng, Y. Guo, J. F. Douglas and W. Xia, Understanding the Role of Cross-Link Density in the Segmental Dynamics and Elastic Properties of Cross-Linked Thermosets, *J. Chem. Phys.*, 2022, **157**(6), DOI: [10.1063/5.0099322](https://doi.org/10.1063/5.0099322).
- 69 J. Shen, X. Lin, J. Liu and X. Li, Effects of Cross-Link Density and Distribution on Static and Dynamic Properties of Chemically Cross-Linked Polymers, *Macromolecules*, 2019, **52**(1), 121–134, DOI: [10.1021/acs.macromol.8b01389](https://doi.org/10.1021/acs.macromol.8b01389).
- 70 C. W. H. Rajawasam, O. J. Dodo, M. A. S. N. Weerasinghe, I. O. Raji, S. V. Wanasinghe, D. Konkolewicz and N. De Alwis Watuthanthrige, Educational Series: Characterizing Crosslinked Polymer Networks, *Polym. Chem.*, 2024, **15**(4), 219–247, DOI: [10.1039/D3PY00914A](https://doi.org/10.1039/D3PY00914A).
- 71 F. Abd-El Salam, M. H. Abd-El Salam, M. T. Mostafa, M. R. Nagy and M. I. Mohamed, Effect of the Vulcanizing System on the Mechanical Properties of Butyl Rubber/Ethylene Propylene Diene Monomer–Carbon Black Blends, *J. Appl. Polym. Sci.*, 2003, **90**(6), 1539–1544, DOI: [10.1002/app.12739](https://doi.org/10.1002/app.12739).
- 72 R. Martin, A. Rekondo, A. Ruiz de Luzuriaga, G. Cabañero, H. J. Grande and I. Odriozola, The Processability of a Poly (Urea-Urethane) Elastomer Reversibly Crosslinked with Aromatic Disulfide Bridges, *J. Mater. Chem. A*, 2014, **2**(16), 5710, DOI: [10.1039/c3ta14927g](https://doi.org/10.1039/c3ta14927g).
- 73 F. Van Lijsebetten, K. De Bruycker, Y. Spiesschaert, J. M. Winne and F. E. Du Prez, Suppressing Creep and Promoting Fast Reprocessing of Vitrimers with Reversibly Trapped Amines, *Angew. Chem., Int. Ed.*, 2022, **61**(9), DOI: [10.1002/anie.202113872](https://doi.org/10.1002/anie.202113872).
- 74 A. Perego and F. Khabaz, Creep and Recovery Behavior of Vitrimers with Fast Bond Exchange Rate, *Macromol. Rapid Commun.*, 2023, **44**(1), DOI: [10.1002/marc.202200313](https://doi.org/10.1002/marc.202200313).
- 75 G. Vozzolo, M. Ximenis, D. Mantione, M. Fernández and H. Sardon, Thermally Reversible Organocatalyst for the Accelerated Reprocessing of Dynamic Networks with Creep Resistance, *ACS Macro Lett.*, 2023, **12**(11), 1536–1542, DOI: [10.1021/acsmacrolett.3c00544](https://doi.org/10.1021/acsmacrolett.3c00544).
- 76 A. Roig, V. D'Agostino, À. Serra and S. De la Flor, Towards Fast Relaxation Rates and Creep Resistance in Disulfide Vitriimer-like Materials, *React. Funct. Polym.*, 2023, **193**, 105764, DOI: [10.1016/j.reactfunctpolym.2023.105764](https://doi.org/10.1016/j.reactfunctpolym.2023.105764).
- 77 F. Van Lijsebetten, T. Debsharma, J. M. Winne and F. E. Du Prez, A Highly Dynamic Covalent Polymer Network without Creep: Mission Impossible?, *Angew. Chem., Int. Ed.*, 2022, **61**(48), DOI: [10.1002/anie.202210405](https://doi.org/10.1002/anie.202210405).
- 78 R. Tang, B. Xue, J. Tan, Y. Guan, J. Wen, X. Li and W. Zhao, Regulating Lignin-Based Epoxy Vitriimer Performance by Fine-Tuning the Lignin Structure, *ACS Appl. Polym. Mater.*, 2022, **4**(2), 1117–1125, DOI: [10.1021/acsapm.1c01541](https://doi.org/10.1021/acsapm.1c01541).
- 79 F. C. Klein, M. Vogt and V. Abetz, Reprocessable Vanillin-Based Schiff Base Vitrimers: Tuning Mechanical and Thermomechanical Properties by Network Design, *Macromol. Mater. Eng.*, 2024, **309**(3), DOI: [10.1002/mame.202300187](https://doi.org/10.1002/mame.202300187).
- 80 B. Li, G. Zhu, Y. Hao, R. Li, X. Zhang and X. Guo, High-performance Epoxy Vitriimer Composites Based on Double Dynamic Covalent Bonds, *J. Polym. Sci.*, 2024, **62**(7), 1468–1479, DOI: [10.1002/pol.20230819](https://doi.org/10.1002/pol.20230819).
- 81 Y. Song, G. Song, J. Li, X. Tang, S. Yin, J. Mai and X. Li, High-efficiency Self-repairing Polyurethane Based on Synergy of Disulfide Bonds and Graded Hydrogen Bonds, *J. Appl. Polym. Sci.*, 2024, **141**(5), DOI: [10.1002/app.54892](https://doi.org/10.1002/app.54892).
- 82 X. Jian, Y. Hu, W. Zhou and L. Xiao, Self-healing Polyurethane Based on Disulfide Bond and Hydrogen Bond, *Polym. Adv. Technol.*, 2018, **29**(1), 463–469, DOI: [10.1002/pat.4135](https://doi.org/10.1002/pat.4135).
- 83 Y. Wang, Y. Li, J. Bai, Z. Li and G. Hu, A Robust and High Self-Healing Efficiency Poly(Urea-Urethane) Based on Disulfide Bonds with Cost-Effective Strategy, *Macromol. Chem. Phys.*, 2019, **220**(23), DOI: [10.1002/macp.201900340](https://doi.org/10.1002/macp.201900340).

